Adsorption 11: 215–227, 2005

Zeolite Membranes: From the Laboratory Scale to Technical Applications*

JÜRGEN CARO
University of Hanover, Institute of Physical Chemistry and Electrochemistry, Callinstr. 3-3A,
D-30167 Hannover, Germany

MANFRED NOACK AND PETER KÖLSCH
Institute for Applied Chemistry Berlin-Adlershof, Richard-Willstätter-Str. 12, D-12489 Berlin, Germany

Abstract. Current trends and novel concepts in R&D of zeolite membranes like the seeding supported crystallization and the preparation of Al-containing zeolite membranes are discussed. The influences of adsorption and diffusion on the permeation properties of zeolite membranes are considered. Dehydration of ethanol by steam permeation and pervaporation as the first zeolite membrane based industrial separation is presented. Membrane supported dehydrogenation and esterification are discussed as possible applications of a catalytic membrane reactors.

Keywords: molecular sieve, zeolite membrane, permeation, pervaporation

1. Introduction

In 1989 Schirmer evaluated the application potential of membranes in industrial separations (Kölsch and Schirmer, 1989). Reflecting the low level of inorganic membrane development at that time, in this review from 1989 only polymeric membranes have been considered on the basis of the solution-diffusion model. Neither inorganic nor organic pore membranes were mentioned in this paper despite the fact that Wolfgang Schirmer was one of the pioneers in the study of the fundamentals of adsorption and diffusion in microporous solids, especially zeolite molecular sieves and their technical application.

The regular pore structure of a molecular sieve suggests that a thin zeolite membrane layer can discriminate between molecules of different size and shape. Due to the interplay of mixture adsorption and mixture diffusion, reasonable separation effects on zeolite membranes can be expected according to specific adsorptive interactions and/or differences in the molecular mobilities. By the end of the 80ies, the idea was born to develop zeolite membranes and the first attempts to prepare zeolite membranes were reported, the first patents were claimed. Parallel to the progress in the preparation of zeolite membranes, the theoretical fundamentals for the molecular understanding of mixture permeation through pore membranes were laid by Barrer (1987, 1990).

In a recent paper, dedicated W. Schirmer on the occasion of his 80th birthday, the state of the art of R&D of inorganic membranes was highlighted (Caro et al., 2000). In a following paper the innovation potential of molecular sieve membranes for industrial applications was discussed (Noack et al., 2002). It is the aim of this paper to analyze the last 15 years of zeolite membrane development and to show future trends.

2. Adsorption Effects Influencing the Permeation Behaviour of Zeolite Membranes

For microporous membranes such as zeolite membranes, the permeation behaviour is determined by the interplay of adsorption and diffusion effects (Caro et al., 2000). However, this superposition of adsorption

---

*In memoriam Wolfgang Schirmer.

and diffusion has to be considered only in the case when more than one component of a mixture is adsorbed by the zeolite membrane according to their size relative to the zeolite pores. Much simpler is the case if we have real molecular sieving, that is to say that one or more components of a mixture are too large to pass the pores of a zeolite membrane (Noack et al., 1994). Permeation can be exactly described by the Maxwell-Stefan-equations for single components (Kapteijn et al., 1994, 1995) and mixtures (Krishna et al., 1995). In contrast to the solubility-diffusivity concept for organic polymer membranes, in pore membranes the adsorption volume is limited and for inorganic pore membranes the pore volume does not noticeable change by swelling. As a consequence, the permeation flux can't increase unlimited when the pressure difference is increased and, therefore, in contrast to organic polymer membranes, the pressure normalized permeance in [mol/m^2 h bar] drops with increasing pressure. The driving force for the permeation process is the concentration gradient across the zeolite layer, grad c. For a given membrane thickness d, grad c can be approximated by the ratio of the concentration difference between the feed and permeate sides of the membrane divided by d. Thus, via the operational pressure on the feed and permeate sides, grad c is determined by the adsorption isotherm. Figure 1 shows for n-butane on a Silicalite I membrane that assuming Langmuir-like isotherms, the membrane with the lowest trans-membrane pressure difference can have the highest driving force, i.e. the largest grad c, when vacuum or sweep gas are applied to reduce the partial pressure of the permeating component on the permeate side of the membrane.

Usually for real zeolite membranes a superimposition of two fluxes is observed: The intracrystalline flux through the regular zeolite pores and an additional flux through narrow mesopores which are only slightly larger than the zeolite pores. The flux through these defect pores in the mesopore range can spoil completely any shape selectivity and result in very low separation factors. For a quantitative evaluation of the flux through the defect pores in the mesopore region permporosimetry can be used. This technique is similar to permporometry (Ash et al., 1963, 1973; Katz and Baruch, 1986; May-Marom and Katz, 1986; Cuperus et al., 1992; Cao et al., 1993), dynamic capillary condensation porometry (Gallaher and Liu, 1994; Lin et al., 1994) or dynamic flow-weighted pore-size distribution technique (Fain, 1994). To the authors knowledge, permporometry which was originally developed for the characterization of pores where the Kelvin equation is valid ($r > 1.5$ nm) was than extended to the microporous membranes (e.g. Julbe and Ramsay, 1996; Steriotis et al., 2000) and first applied to zeolite membranes by Deckman et al. (2001) and further developed by different groups (see e.g. Noack and Caro, 2002; Caro, 2002; Beltsios et al., 2002). In this method the permeation flux of an inert gas such as helium or nitrogen is measured in the presence of a second strongly adsorbing gas which can completely fill and block even at low partial pressures the regular zeolite pores. The highly adsorbing gas such as n-hexane or water is mixed to the inert gas with increasing p/p_s ratios. According to the Kelvin equation, at a certain p/p_s ratio the zeolite pores are filled and the remaining flux of the inert gas can be contributed exclusively to non-regular zeolite mesopores. When the p/p_s ratio of the strongly adsorbing component is continuously increased, mesopores of increasing diameters become filled and so blocked for the flux of the inert gas. The adsorption isotherm indicates whether a molecule is suitable as strongly adsorbing component (Fig. 2).

The n-hexane molecule with a kinetic diameter of 0.43 nm can easily adsorb into the MFI pores and shows at room temperature a steep slope in the adsorption isotherm reaching the saturation adsorption capacity between $p/p_s = 0.1$ to 0.9. Cyclohexane with a kinetic molecule diameter of 0.62 nm is larger than the MFI-pore diameter of 0.55 nm which results in relative low amounts adsorbed. The small water molecule with 0.26 nm diameter has only a weak interaction with the hydrophobic SiO_2 pore surface of Silicalite I and reaches only 5% of the saturation capacity of n-hexane. Therefore, water and cyclohexane are no suitable probe molecule for blocking the zeolite pores of a Silicalite I membrane for permporosimetry.

Figure 3 shows an example for a permporosimetric measurement using nitrogen as the non-adsorbing gas and n-hexane as the strongly adsorbing probe molecule. Three different MFI membranes were studied and the results of permporosimetry are compared with permeation experiments for n/i-pentanes (50%/50%) mixtures. The nitrogen permeance through the non-hexane loaded membranes was set 100%. The decreases of the nitrogen flux is the result of the zeolite pore blocking by the strongly adsorbing component n-hexane. The MFI membrane with the highest n/i selectivity of 58.1 is the Silicalite I membrane where the nitrogen flux is reduced to $<0.2\%$ at the n-hexane $p/p_s = 0.1$. For

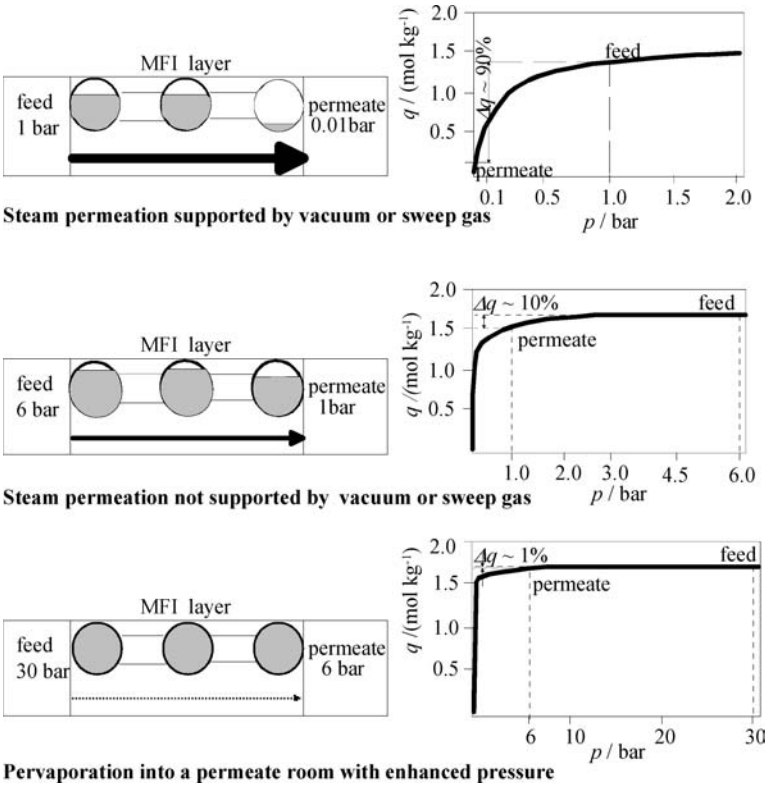

Steam permeation supported by vacuum or sweep gas

Steam permeation not supported by vacuum or sweep gas

Pervaporation into a permeate room with enhanced pressure

Figure 1. Schematic representation of the consequences of different operational pressures on the feed and permeate sides of a Silicalite I membrane. The differences of the *n*-butane loadings on the feed and permeate sides of an MFI membrane as driving force for the permeation flux are estimated from the adsorption isotherms of butane at 135°C on Silicalite I. The flux intensity is indicated by arrows of different thickness (after Noack and Caro, 2002, with permission from Elsevier).

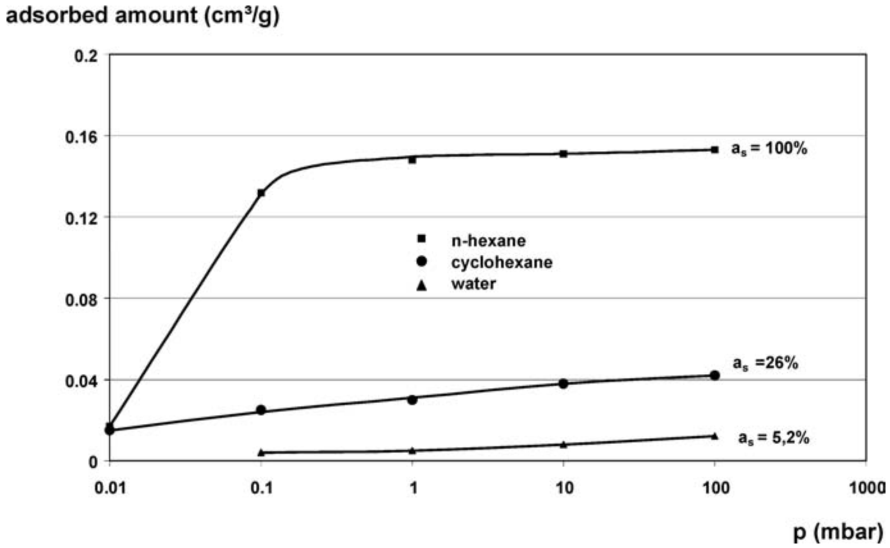

Figure 2. Adsorption isotherms of *n*-hexane, cyclohexane and water on Silicalite I (Si/Al ≈ 300) at $T = 25°\mathrm{C}$ (after Lohse et al., 1987) showing the influence of hydrophilic/hydrophobic interactions and the molecule size on the amount adsorbed. In permporosimetry the range of measurement is at $p/p_s = 0.01 \ldots 0.5$ of the strongly adsorbed component (cf. Fig. 3).

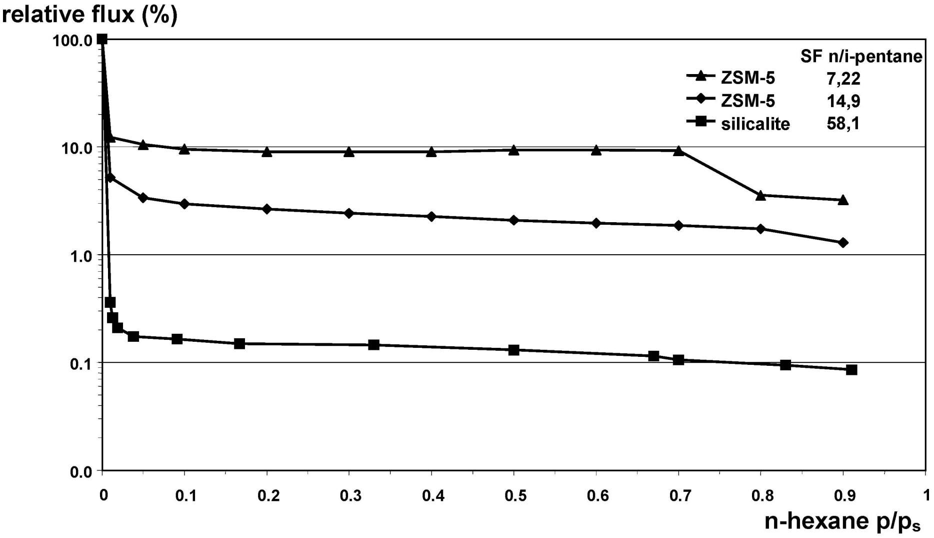

Figure 3. Permporosimetry showing the reduction of a nitrogen flux through three MFI membranes of different Si/Al as a function of the partial pressure of *n*-hexane at 25°C. The remaining N_2 flux through defect pores correlates with the separation factor SF for a 50%/50% *n*/*i*-pentane mixture. The two ZSM-5 membranes of the same Si/Al = 270 were prepared in rotating autoclaves: For ▲ the autoclave was 70% filled with gel and the membrane layer was crystallized on the shell side of the ceramic tube; for ◆ the autoclave was completely filled and the membrane layer was crystallized on the tube side.

the two different ZSM-5 membranes the nitrogen flux at the *n*-hexane $p/p_s = 0.1$ was reduced only to 3% and 10% which is a clear indication for the existence of still unblocked mesopores. It turned out as a finger print of a highly selective MFI membrane, that at hexane $p/p_s = 0.1$ the relative flux of the inert gas should be less than 10%. Consequently, the *n*/*i*-pentane mixture separation factors measured for the two ZSM-5 membranes were only 14.9 and 7.2, respectively. In chapter 4 of this paper it will be shown that the concentration of mesopores increases with the Al content of the MFI membrane.

3. Diffusion Effects Influencing the Permeation Behaviour of MFI Membranes

During the last few years for the controlled preparation of supported zeolite membranes seeding techniques (secondary growth) have been established. By decoupling the nucleation step (at high supersaturation) from crystal growth (at low supersaturation), the seeds can grow in low concentrated solutions under suppression of secondary nucleation. To the authors knowledge, the first patent to seed a support surface was submitted in 1994 (Lai et al., 1994), the first paper appeared in 1993 (Horii et al., 1993). There are two established methods to attach the seeds to the surface of the support by using the different zeta-potentials of the support and seed crystal surfaces: (i) Tsapatsis et al. change the pH of the solution to adjust different zeta potentials between the ceramic support (e.g. α-Al_2O_3) and the SiO_2 seeds (e.g. Silicalite I) (Lovallo et al., 1998; Gouzinis and Tsapatsis, 1998; Xomeritakis et al., 1999). (ii) Sterte and co-workers adsorb cationic oligomers/polymers on the support to create a positive surface charge and the negatively charged zeolite seeds such as Silicalite I become attached (Hedlund et al., 1997; Mintova et al., 1997; 1998). Later this method which was first developed for coating Si wafers, was successfully transformed for seeding porous ceramic supports for membrane preparation (Hedlund et al., 1999).

By the seeding of the support, MFI membrane layers of different crystallographic orientation can be obtained. MFI-type zeolite membranes often show a crystallographic orientation of the *c*-axis of the zeolite layer perpendicular to the plane of the support surface (Nair et al., 2001; Wong et al., 2001). Under certain growth conditions other crystallographic orientations were observed like a-orientation (Hedlund et al., 1999; Wang and Yan, 2001), *b*-orientation (Koegler et al., 1997; Lai et al., 2002) or intermediate orientations (Tanaka et al., 2002; Bons and Bons, 2003).

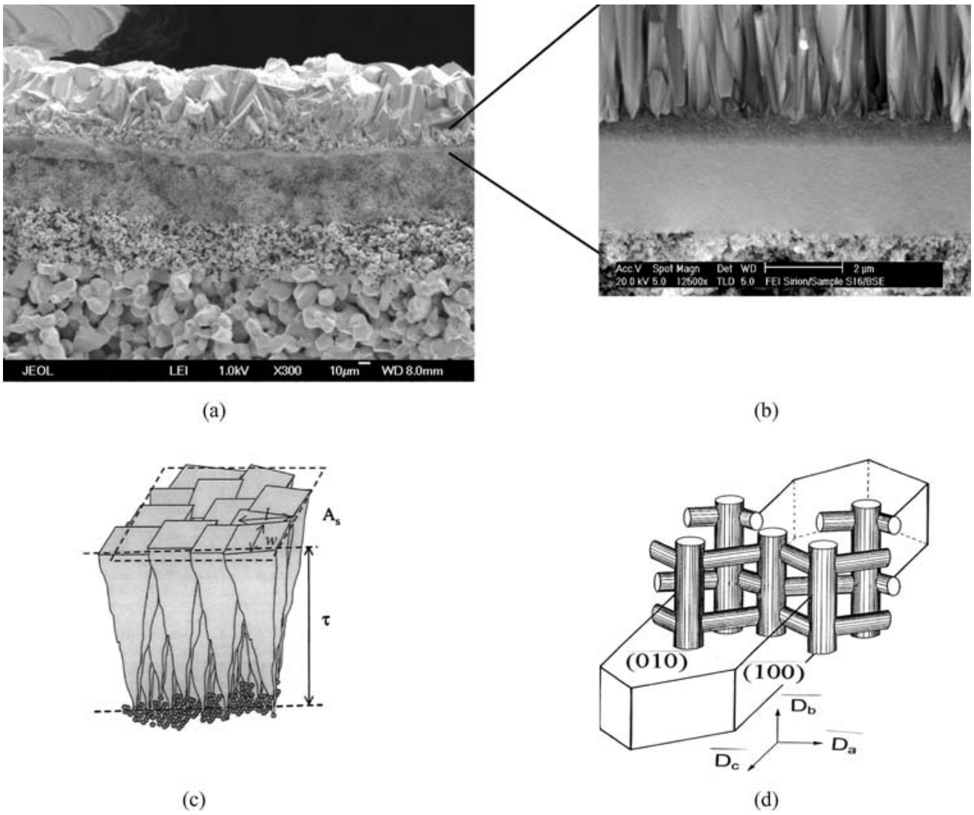

Figure 4. Typcial polycrystalline MFI (Silicalite I) layer on the inner surface of a 1 cm tubular alumina support with asymmetric structure prepared by seeded crystallization (after Noack et al., 2001) (a). The Silicalite I crystals start to grow from the seed layer resulting in a columnar growth structure (b). Scheme of the development of the crystallographic *c*-orientation by the evolutionary growth selection model (from Wong et al., 2001, with permission from Elsevier) (c). Anisotropy of the MFI pore structure and the resulting anisotropy in mass transport expressed by the diffusion tensor elements D_a, D_b and D_c (d).

The *c*-orientation can be explained by the competitive growth model. If the crystal growth is anisotropic and we have randomly oriented seeds, those crystallites with their fastest growth direction pointing away from the seeded surface will grow more rapidly than crystallites in other orientations. Finally, the crystals with the fastest growth direction perpendicular to the plane of the membrane will dominate. For MFI crystals usually the *c*-axis is the longest dimension and, consequently, the *c*-axis is the fastest growth direction. Therefore, most MFI-membranes are *c*-oriented with a columnar structure as shown in Fig. 4.

From the study of the diffusion anisotropy of the MFI structure it can be expected, that permeation through *c*-oriented MFI membranes is less favourable (Caro et al., 1993). A *b*-oriented MFI layer is expected to exhibit higher fluxes. Recently, Tsapatsis and co-workers have prepared a b-oriented MFI Silicalite I membrane (Lai et al., 2003). They used relative large seeds ($0.5 \times 0.2 \times 0.1\ \mu m^3$) and attached the seeds as an *b*-oriented monolayer to the support surface. By using di- and trimers of tetrapropylammoniumhydroxide (TPAOH) the growth of the seeds in *b*-direction could be enhanced. The resulting polycrystalline films are 1 μm thin and consist of large *b*-oriented single crystals with straight channels running down the membrane thickness. This very careful membrane preparation results in a superior separation performance which was demonstrated for the xylene isomers separation.

The development of high-flux and high-selectivity MFI membranes for the xylene separation by the Tsapatsis group (Lai et al., 2003) shows the importance of a certain channel orientation and the significance of a seeded growth of an oriented particle monolayer.

Whereas a *c*-orientation results in a separation factor[1] SF ≈ 1, the *b*-orientation gives a xylene SF ≈ 500 at 200°C. It is interesting to note that in the latter case the SF increases with increasing temperature. This experimental finding is characteristic of the interplay of adsorption and diffusion effects. At low temperatures the zeolite pores are filled to a certain degree and we have a *single file* like behaviour. That is to say that the more mobile *p*-xylene cannot move faster through the pore network than the less mobile *o*-xylene. This situation changes dramatically at lower pore filling which is found at higher temperatures and/or lower partial pressures. Now the mobile p-xylene can move more or less independently from the presence of *o*-xylene. The permeation experiments were carried out at very low loadings according to low summar xylene pressures $p/p_s \approx 0.007$ due to a high content of inert gas in the feed stream and the high temperature.

4. New Concepts in Zeolite Membrane Preparation

The International Zeolite Association (IZA) data base contains more than 152 different zeolite structures. It is estimated that about 15 structures have been tried to prepare as a zeolite membrane. It was found experimentally that only the high-silica types showed shape-selective separation behaviour, especially Silicalite I as the Al-free MFI structure. Most progress in the development of molecular sieve membranes was achieved for Silicalite I membranes since their preparation is relatively easy. This highly siliceous zeolite provides chemical stability and allows oxidative regeneration (Noack and Caro, 2002). So far, under lab-scale conditions only these high-SiO_2 zeolite membranes show clear molecular sieving. When the high Al-containing zeolite membranes are tested in shape selective gas or steam permeation, usually Knudsen separation pattern is found which indicates the contribution of high meso- and macropore mass transport. However, the successful application of LTA membranes in dehydration is primarily based on differences in the mixture adsorption behaviour rather than in the molecular size and can tolerate, therefore, minor membrane defects. In a recent paper (Feibelman, 2004) the experimental finding is reported that water becomes extremely immobilized in narrow pores of oxide materials because of strong hydrophilic interaction with the oxide surface. This phase of "frozen" water could effectively block mesopores in LTA membranes thus increasing their selectivity.

It seems to be a general problem to crystallize thin defect-free Al-containing MFI layers as shown by recent papers (Noack et al., 2005; 2005). This idea is supported by the measurement of the zeta potential of MFI zeolites of different Si/Al suspended in water (Noack and Stelzer, 2004). Figure 5 shows the common tendency that the surface charge of the zeolite is the more negative the higher the Al content is. It is assumed that the negative surface charges suppress the growth of the Al-containing seeds to a continuous defect-free zeolite layer because of the relative high negative surface charge. It is proposed, therefore, to give a positively charged additive to the crystallization batch which is adsorbed at the growing seed crystals to compensate their negative surface charge. In our experiments hexamethyl-ethylen-diammonium dijodide (HMEDA) was used as this additive. HMEDA was not incorporated into the growing zeolite layer during the synthesis and it did not alter the Si/Al ratio in the zeolite layer compared with the HMEDA-free membrane preparation. Table 1 shows that the use of HMEDA gives MFI (ZSM-5) membranes with lower concentrations of non-zeolite mesopore defects demonstrated by the (i) decrease of the H_2 flux and the (ii) increase of the permselectivity as the ratio of the single component fluxes in comparison with the HMEDA-free membrane synthesis.

5. Zeolite Membranes in Membrane Reactors

There are numerous examples of the application of zeolite membranes to enhance a chemical reaction

Table 1. Influence of the addition of hexamethyl-ethylen-diammonium dijodide (HMEDA) on the formation of defect pores in MFI (ZSM-5) membrane crystallisation (Si/Al = 96). The synthesis composition was $SiO_2 : TPAOH : TPABr : NaOH : Al_2O_3 : H_2O = 100:3.33:3.33:6.67:0.526:2000$, the synthesis conditions were 180°C, 48 h. The HMEDA-concentration in the synthesis batch was 0.01 molar. Permeation measurements at 105°C.

	Without HMEDA	With HMEDA
H_2 permeance in l/m^{2}hbar	957	450
permselectivity H_2O/propanol	7.3	35.6

---

[1] Separation factor SF = ($x_{\text{p-xylene,permeate}} : x_{\text{o-xylene,permeate}}$) : ($x_{\text{p-xylene,retentate}} : x_{\text{o-xylene,retentate}}$) with x denoting the mole fraction.

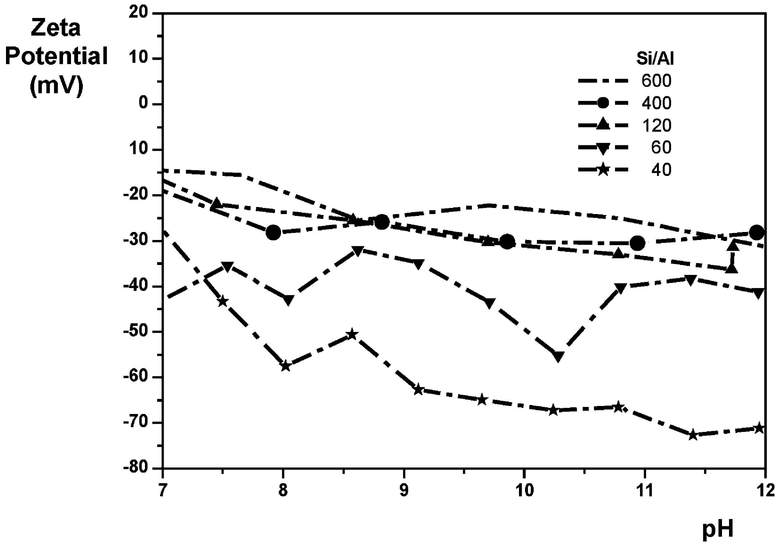

Figure 5. Zeta-potential for MFI zeolites of different Si/Al ratios suspended in water at room temperature as a function of the pH (Noack and Stelzer, 2004, measurements by Malvern Zeta Sizer).

like dehydrogenation, partial oxidation or isomerization. However, in only a few of these cases the zeolite membrane acts as a real shape- and size-selecting molecular sieve. In the following example it will be shown that an MFI zeolite membrane can be used in catalytic dehydrogenations despite the fact that both H_2 and *i*-butane can pass the 0.55 nm pores due to their kinetic diameters (0.29 nm and 0.50 nm, resp.).

Whereas at low temperatures the separation of a hydrogen/*i*-butane mixture is adsorption-controlled and the membrane is *i*-butane-selective ($SF_{H_2:i\text{-butane}} \ll 1$), Fig. 6 shows that with increasing temperatures, the permeation becomes diffusion-controlled and the membrane shows hydrogen-selectivity ($SF_{H_2:i\text{-butane}} \gg 1$). A similar observation of a temperature inversion of the membrane selectivity was observed for the mixture methane/*n*-butane on silicalite I: At room temperature the silicalite I membrane was found to be methane-selective, at 350°C it was butane-selective (Geus et al., 1993). The reasonable H_2-selectivity of an $SF \approx 70$ (Fig. 6) with a permeance of about 1 Nm^3 H_2/m^2 h bar at 500°C suggests that this MFI membrane could enhance dehydrogenations in a membrane reactor by selective H_2 removal. It is remarkable, that no degradation during one week of operation at 500°C including 5 oxidative regenerations to burn off carbonaceous residues was observed (Illgen et al., 2001).

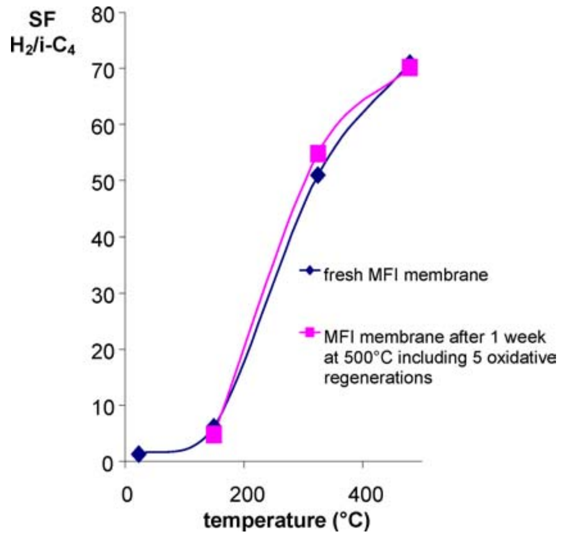

Figure 6. Mixture separation factor SF for H_2:*i*-butane (feed composition 1:3 which is representative for the equilibrium composition of the *i*-butane dehydrogenation at 500°C) for different temperatures.

Figure 7 represents the comparison of the *i*-butane conversion in the classical fixed bed with the membrane reactor. The comparison was made in an identical reactor with and without H_2-removal as reference experiment called “classical fixed bed”. In the classical fixed bed experiment the thermodynamic equilibrium

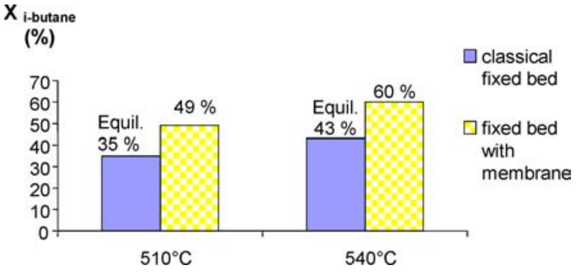

Figure 7. Increase of the *i*-butane conversion X above the equilibrium in a catalytic dehydrogenation if the hydrogen is drained off by the MFI membrane. WHSV = 1 h^{-1}, Cr_2O_3 on Al_2O_3 (Sued-Chemie), 20 cm^2 membrane area/g catalyst, data after 20 min time on stream (after Illgen et al., 2001, with permission of Elsevier).

conversions have been obtained. When the hydrogen was removed from the shell side of the reactor by a sweep gas or vacuum, the conversion increased by about 15%. This removal of the hydrogen has two positive effects in comparison with the classical fixed bed: (i) the conversion of the i-butane is increased and (ii) the selectivity of the *i*-butene formation increases since the hydrogenolysis is suppressed. As a result, at the beginning of the reaction the *i*-butene yield in the membrane reactor is by ca. 1/3 higher than the classical fixed bed. However, as a result of the hydrogen removal, coking is promoted and after ca. 2 h time on stream the olefin yield of the membrane reactor drops below that of the classical fixed bed (Schäfer et al., 2003). After an oxidative regeneration the activity and selectivity are restored completely.

In the second example the effect of water removal during an esterification will be shown. There are different ways to increase the yield of an esterification. Most frequently of cheapest educt is present in a surplus concentration or the low boiling ester is removed by reactive distillation. Another concept is to keep the concentration of the product molecule water as low as possible by the use of adsorbents like LTA zeolites or even by chemical reactions like the hydrolysis of Al tri-isopropylate. In this paper the use of hydrophilic membranes is proposed. In the case of the low-temperature esterification of methanol or ethanol with short chain monovalent hydrocarbon acids, hydrophilic organic polymer membranes can be used for the dewatering. However, to support esterifications at higher temperatures, hydrophilic inorganic membranes with high stability against strong acids have to be used. MFI type zeolite membranes are suitable candidates to fulfil these demands. Figure 8 shows that the water/*i*-propanol permselectivity as function of the Si/Al of the MFI membranes studied passes a maximum at Si/Al = 119. This maximum is the result of the interplay of two contradicting effects. On the one hand side, high Al concentrations in the MFI membrane increase the hydrophilicity and, thus, the water/alcohol selectivity. On the other hand, high Al concentrations increase the mesopore concentration in the MFI membrane as one can see from the high H_2 flux at low Si/Al ratios.

Figure 9 shows the benefits of a membrane supported esterification of *n*-propanol with propionic acid using an MFI membrane of the Si/Al = 96. For infinite reaction time, the ester yield can be increased from 52% to 92% by removal of water through the membrane. This MFI membrane of Si/Al = 96 is acid stable up to

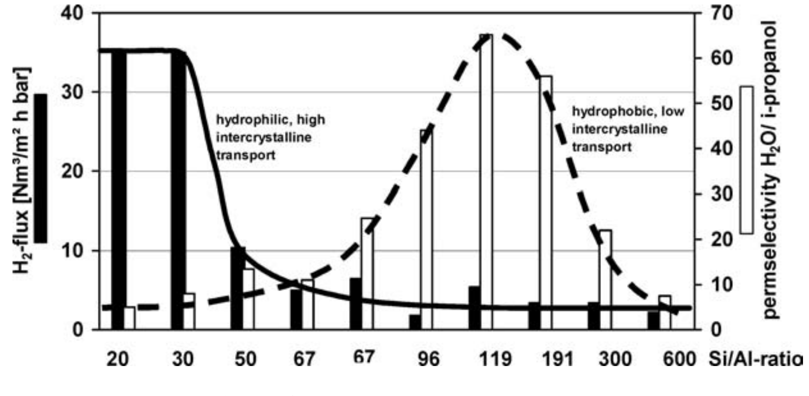

Figure 8. Correlation between the Si/Al ratio of ZSM-5 type MFI membranes and the existence of mesopores, detected by the H_2 flux (left ordinate). Maximum of the permselectivity H_2O/*i*-propanol as a function of the Si/Al ratio according to the interplay of hydrophilic interaction and the existence of defect pores (right ordinate). The permselectivity is derived as the ratio of the single component fluxes in steam permeation. All measurements at 105°C.

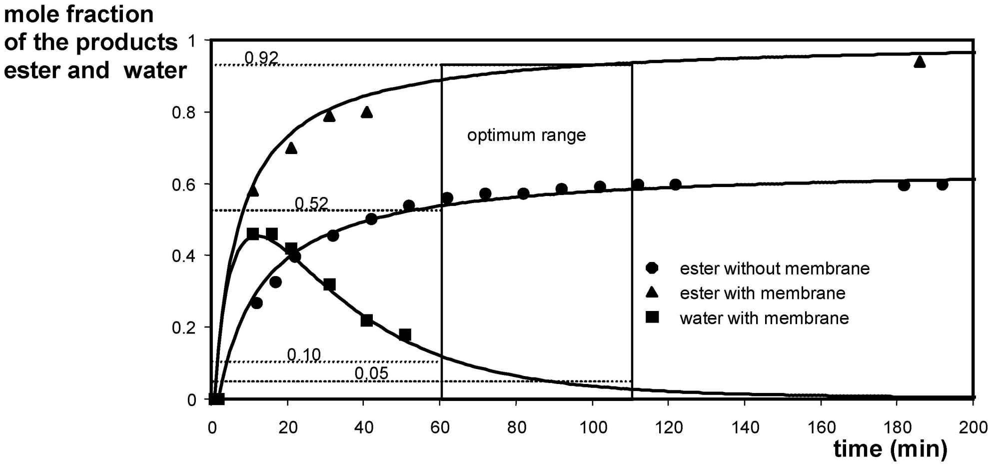

Figure 9. Influence of an MFI membrane with Si/Al = 96 on the increase of the yield as a function of the reaction time in the esterification of propionic acid and *i*-propanol at 70°C. The optimum working range for the dewatering by pervaporation is given for a water concentration between 5 and 10% water in the reaction mixture.

pH = 1 but—due to the low Al contents—the hydrophilicity is low and, consequently, the resulting water flux of 72 g/m^2 h bar is still too low for technical applicatons.

6. Industrial Application of LTA Membranes in Ethanol Dehydration

Commercial zeolite membranes sold by the Japanese companies Mitsui Engineering & Shipbuilding Co. and the Nano-Research Institute Inc. (XNRI), a 100% subsidiary of Mitsui & Co., and most recently by the European alliance between Smart (U.K.) and Inocermic (Germany) consist of a hydrophilic LTA zeolite layer on a ceramic tubular support and are extremely selective in the separation of water from organic solutions by steam permeation and pervaporation. As a crystalline material, zeolites are much more stable towards phase transformation and densification compared with X-ray amorphous metal oxide membrane layers from sol-gel techniques. However, because of the high Al content, LTA membranes should be operated at $6.5 < \mathrm{pH} < 7.5$.

XNRI has installed vapour permeation units in Brazil (3,000 l/d) (see Fig. 10) and India (30,000 l/d) at an operation temperature of 130°C for the dewatering of bio ethanol using LTA membranes. In laboratory tests at 75°C the membrane performance for a 90% ethanol/10% water test mixture was determined to be 8 kg H_2O/m^{2}h with a separation factor $SF_{H_2O/\mathrm{ethanol}} \approx 10{,}000$. Nevertheless, in the industrial plant the permeate was not pure water but it contained 0.5 to 1.0% ethanol. The ethanol concentration in the feed is 93%, in the retentate it is 99.7%. The demonstration plant in Brazil is driven by electricity applying vapour compressor energy recycling. In the industrial 30,000 l/d plant which was installed in Jan. 2004 at Daurala Sugar Works near New Delhi, the feed is evaporated by heating with steam. The operating pressure and temperature of the membrane are 600 kPa and 130°C, respectively (Ikeda, 2004). Very recently XNRI announced the development of a high flux faujasite membrane of types X and Y on tubular alpha alumina support. Compared with the corresponding LTA membranes the faujasite ones are chemically more stable. For a test mixture of water (10 mass%) and ethanol (90 mass%) at 75°C fluxes of 6–9 kg/m^{2}h with a separation factor of 100–400 can be achieved for the X type and about 4 kg/m^2 h with a separation factor of about 150 for the Y type (Ikeda, 2004).

In alliance between Smart Chemicals Development and Inocermic GmbH supported membranes of type LTA are produced in a half-industrial scale in Germany (cfi, 2003) (see Fig. 11). The membrane layer is inside an α-Al_2O_3 4-channel-support thus protected against mechanical damage. Organic solutions can be dried to water levels down to 0.1% by pervaporation. A first plant for organic solvent dehydration was commissioned in the UK, a second one with 100 m^2 membrane area bio ethanol dehydration is under construction.

An opposite target can be the continuous removal of ethanol from the fermentation mixture since the

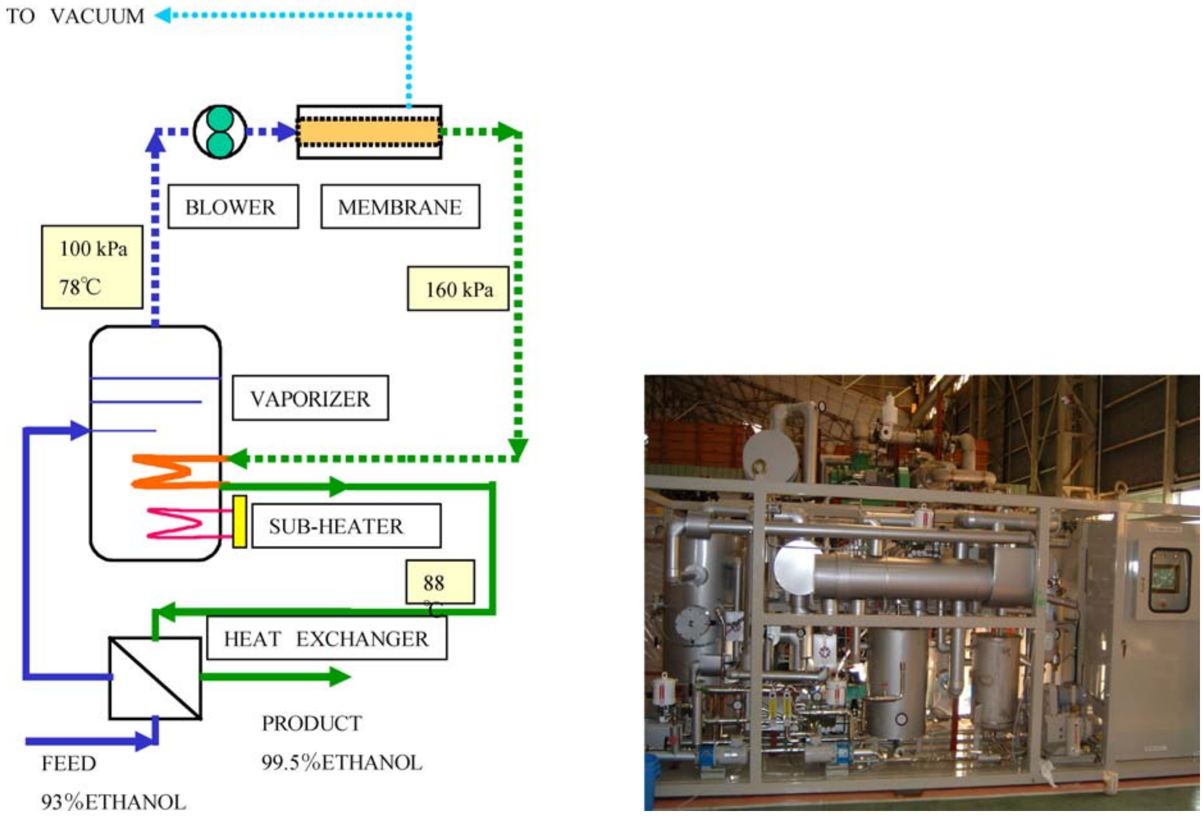

Figure 10. Mitsui demonstration plant in Brazil for the dehydration of bio ethanol by steam permeation using LTA membranes (Ikeda, 2004).

fermentation process stops at ethanol concentrations near 15%. Hydrophobic membranes such as Silicalite I type MFI membranes are in development to solve this problem.

7. New Membranes and New Module Concepts

Most of the recent R&D on zeolite membranes is focussed on the types LTA and MFI. In addition to the interaction-selective hydrophilic LTA membranes, shape-selective MFI membranes are near to a commercialization in the isomer separation like the xylenes (NGK, 2002) or *n*/*i*-hydrocarbons. Recently NGK announced the commercialization of a DDR-type zeolite membrane with narrow pores of $0.36 \times 0.44\,\text{nm}$ openings for CO_2 separation from CH_4 (NGK, 2004). The gas separation characteristics of DDR-type zeolite membranes are reported (Tomita et al., 2004). Also ExxonMobile is active in the field of DDR membranes (Clark et al., 2003). Recently, joint communications of ExxonMobile and NGK on DDR zeolite membranes can be found (Chance et al., 2004).

To reduce the mass flow resistances, high-fluxes membranes of asymmetric cross section as shown in Fig. 4 have been developed. However, a disadvantage of the layered structure of these asymmetric ceramic membranes is the fact that these membranes have to be fired after each layer deposition which increases the production costs. The price of a zeolite membrane is governed, therefore, by the production costs of the support rather than by the zeolite layer. Regarding inocermic GmbH (Germany) as one of the most prominent suppliers of high quality supports and LTA-membrane producer the ceramic support is responsible for at least 70% of the zeolite membrane price. There is a search, therefore, for cheaper and automatic production of membrane supports which can be coated subsequently by functional layers like zeolites,

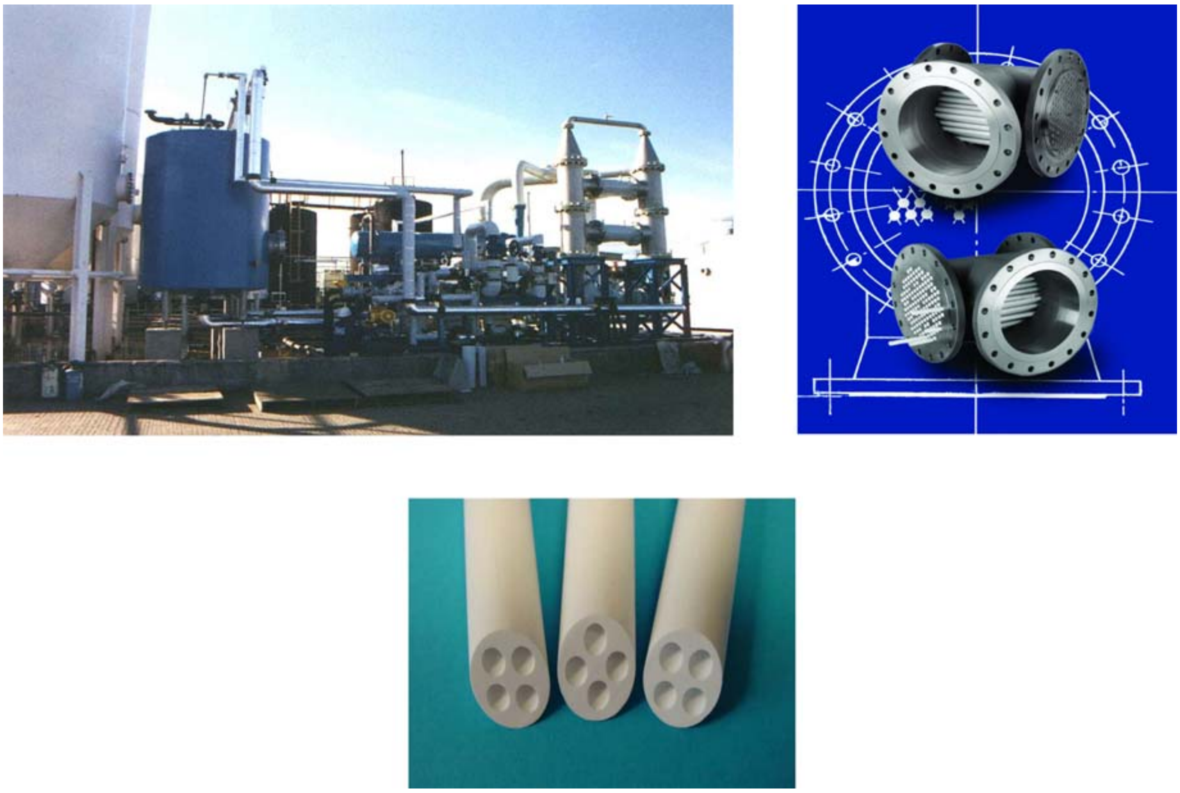

Figure 11. Semi technical pervaporation plant for the dehydration of ethanol in the UK. The modules of 5.8 m^2 membrane area each are equipped with 4-channel Smart zeolite membranes produced by the inocermic GmbH, Germany (inocermic, 2004).

Pd, perovskite or carbon. Figure 12 shows some recent developments.

Another problem to be solved is the module design. An advantage of inorganic membranes compared with polymeric ones is the high temperature stability of the inorganic membranes which allows e.g. an in situ oxidative regeneration. To keep this advantage, inorganic membranes should be sealed into modules by avoiding organic polymers. A new solution is the full ceramic module shown in Fig. 13 where tubular membranes are potted by a ceramic binder. In the case of zeolite membranes this technology requires the seeding and zeolite layer growth after completion of the housing.

8. Outlook

Since inorganic membranes are about 10–50 times more expensive than the equivalent polymeric ones, this cost differential can be tolerated only by unique applications where the polymer membranes fail. Such unique properties of zeolite membranes are their (i) size and shape selective separation behaviour and their (ii) thermal and chemical stability.

LTA membranes in the dewatering of alcohol by steam permeation or pervaporation have reached the commercial state. MFI membranes in shape selective separations are in pilot scale. New and combined permeation methods such as permeation experiments of single components and mixtures with and without pressure difference across the membrane together with permporosimetry give a better insight in the membrane properties and the possibility to improve the membrane preparation.

On the other hand, little progress is seen in the development of small pore zeolite membranes for H_2 separation and zeolite membranes for chiral separations. With the development of capillaries, fibres and multi-channel modules the membrane area to module volume ratio could be improved. Full-ceramic modules can solve the high-temperature sealing. Such separation problems as paraffin/olefin, CO_2/other gases and aromatics/aliphatics can be solved using zeolite membranes.

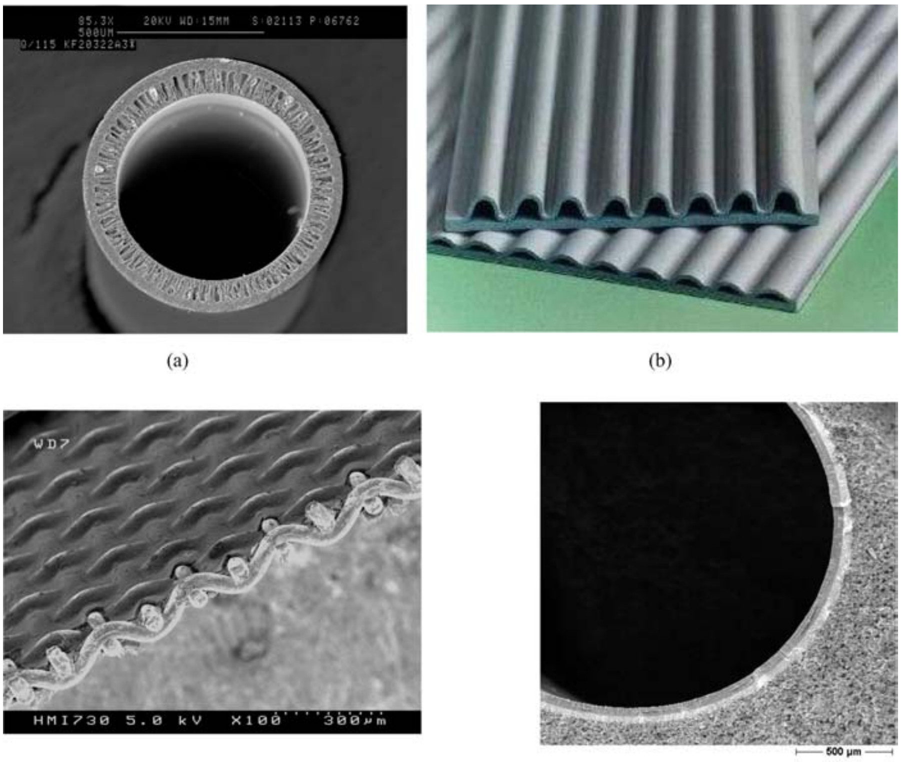

(a) (b)

(c) (d)

Figure 12. Al_2O_3 hollow fibre prepared by a wet spinning process with a wall thickness of about 120 μm, 46% porosity, mean pore size 0.45 μm, bending strength 105 MPa (Goldbach et al., 2001; Kilgus et al., 2004) (a), SiC multi-channel element which can be continuously produced and calcined by cofiring (ikts, 2004) (b), Flexible ceramic foil with a stainless steel web as mechanical support for the ceramic particles (Creavis, 2004; Separion, 2004) (c), and ceramic capillary inside coated with a ZSM5-membranes layer (Richter et al., 2003) (d).

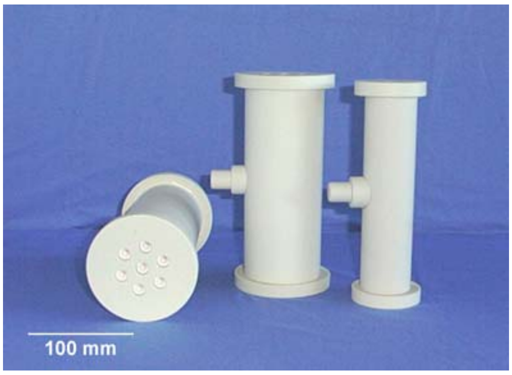

Figure 13. Full ceramic module of the Hermsdorf Institute of Technical Ceramics (Hitk, 2004).

Acknowledgments

We thank for financial support of the projects no. 03C30120 by the Federal Ministry of Education, Science, Research and Technology of Germany, the Senate of Berlin, Department of Science, Research and Culture and the European Union as well as for the financial support of the Deutsche Forschungsgemeinschaft DFG for the grant Ca 149/1.

References

Ash, R., R.M. Barrer, and C.G. Pope, *Proc. Royal Soc. Lond. A*, **271**, 19 (1963).

Ash, R., R.M. Barrer, and R.T. Lowton, *J. Chem. Soc. Farad. Trans.*, **1**, 2166 (1973).

Barrer, R.M., *Langmuir*, **3**, 309 (1987).

Barrer, R.M., *J. Chem. Soc. Faraday Trans.*, **86**, 1123 (1990).

Beltsios, K.G., Th.A. Steriotis, K.L. Stefanopoulos, and N.K. Kanellopoulos, in F. Schüth, K.S.W. Sing, and J. Weitkamp (Eds.). *Handbook of Porous Solids*, Wiley-VCH, ISBN 3-527-30246-8, p. 2382, 2002.

Bons, A.J. and P.D. Bons, *Micropor. Mesopor. Mater.*, **62**, 9 (2003).

Cao, G.Z., J. Meijerink, H.W. Brinkman, and A.J. Burggraaf, *J. Membr. Sci.*, **83**, 221 (1993).

Caro, J., M. Noack, J. Richter-Mendau, F. Marlow, D. Petersohn, M. Griepentrog, and J. Kornatowski, *J. Phys. Chem.*, **97**, 1385 (1993).

Caro, J., in *Handbook of Porous Solids*, F. Schüth, K.S.W. Sing, and J. Weitkamp (Eds.). Wiley-VCH, ISBN 3-527-30246-8, p. 363, 2002.

Caro, J., P. Kölsch, M. Noack, R. Schäfer, I. Voigt, G. Fischer, P. Puhlfürß, and H. Richter, *Chem. Technik*, **52**, 23 (2000).

Caro, J., M. Noack, P. Kölsch, and R. Schäfer, *Micropor. Mesop. Mater.*, **38**, 3 (2000).

cfi, Ber. DKG, **80**(8), E23 (2003).

Chance, R., C. Yoon, T. Clark, H. Deckman, E. Thomas, K. Geurts, P. Rubas, T. Tomita, K. Nakayama, H. Sakai, and K. Suzuki, *Proc. 8th International Congress on Inorganic Membranes, Membrane Synthesis and Characterization* I-4, Connecticut, 2004.

Clark, T., C. Yoon, H. Deckman, R. Chance, D. Ruthven, B. Bonekamp, and P. Pex, *Proc. 14th Annual Meeting of the North American Membrane Society*, Jackson Hole, WY, 2003.

Creavis: http://www.degussa.com.de/innovationen/creavis/keramische_membranen.html, 2004.

Cuperus, F.P., D. Bargeman, and C.A. Smolders, *J. Membr. Sci.*, **71**, 57 (1992).

Deckman, H.W. et al., *Int. Workshop on Zeolitic and Microporous Membranes*, Purmerend, The Netherlands, p. 9, 2001.

Feibelman, P.J., *Langmuir*, **20**, 1239 (2004).

Fain, D.E., *Proc. 1st Int. Conf. Inorg. Membr. Montpellier*, France, p. 199, 1989.

Gallaher, G.R. and P.K.T. Liu, *J. Mater. Sci.*, **92**, 29 (1994).

Geus, E.R., H. van Bekkum, W.J.W. Bakker, and J.A. Moulijn, *Micropor. Mater.*, **1**, 131 (1993).

Goldbach, A., T. Mauer, and N. Stroh, *Keram. Z.*, **53**, 223 (2001).

Gouzinis, A. and M. Tsapatsis, *Chem. Mater.*, **10**, 2497 (1998).

Hedlund, J., B.J. Schoeman, and J. Sterte, *Stud. Surf. Sci. Catal.*, **105**, 2203 (1997).

Hedlund, J., S. Mintova, and J. Sterte, *Micropor. Mesopor. Mater.*, **28**, 185 (1999).

Hedlund, J., M. Noack, P. Kölsch, D. Creaser, J. Caro, and J. Sterte, *J. Membr. Sci.*, **159**, 263 (1999).

hitk: http://www.hitk.de (2004).

Horii, K., K. Tanaky, K. Kita, and K. Okamoto, *Proc. 26th Autumn Meeting of Soc. Chem. Eng.* Japan, **99** (1993).

Ikeda, S., *General Manager XNRI, Bussan Nanotech Research Institute*, Mitsui & Co., Ltd, Personal Communication, 2004.

ikts: http://www.ikts.fhg.de/business/strukturkeramik/verfahren/giessformgebung, 2004.

Illgen, U., R. Schäfer, M. Noack, P. Kölsch, A. Kühnle, and J. Caro, *J. Catal. Commun.*, **2**, 339 (2001).

inocermic: http://www.inocermic.de, 2004.

Julbe, A., and J.D.F. Ramsay, in A.J. Burggraaf and L. Cot (Eds.). *Fundamentals of Inorganic Membrane Science and Technology*, Elsevier, ISBN 0-444-81877-4, p. 67, 2000.

Kapteijn, F., W.J. Bakker, G. Zheng, and J.A. Moulijn, *Micropor. Mater.*, **3**, 227 (1994).

Kapteijn, F., W.J. Bakker, G. Zheng, J. Poppe, and J.A. Moulijn, *Chem. Eng. J.*, **57**, 145 (1995).

Katz, M.G. and G. Baruch, *Desalination*, **58**, 199 (1986).

Kilgus, M., C. Tablet, N. Dinges, D. Senftleben, and T. Schiestel, *Euromembrane*, Hamburg, Germany, 2004.

Koegler, J.H., H. van Bekkum, and J.C. Jansen, *Zeolites*, **19**, 262 (1997).

Kölsch, P. and W. Schirmer, *Chem. Techn.*, **41**, 369 (1989).

Krishna, R., L.J.P. van den Broeke, F. Kapteijn, and J.A. Moulijn, *Chem. Eng. J.*, **57**, 155 (1995).

Lai, W.F., H.W. Deckman, J.A. McHenry, and J.P. Verduijn, US Patent 5,871,650, filed on July 8, 1994.

Lai, S.M., L.T.Y. Au, and K.L. Yeung, *Micropor. Mesopor. Mater.*, **54**, 257 (2002).

Lai, Z., G., Bonilla, I. Diaz, J.G. Nery, K. Sujaoti, M.A. Amat, E. Kokkoli, O. Terasaki, R.W. Thompson, M. Tsapatsis, and D.G. Vlachos, *Science*, **300**, 456 (2003).

Lin, C.L., D.L. Flowers, and P.K.T. Liu, *J. Membr. Sci.*, **92**, 45 (1994).

Lohse, U., H. Thamm, M. Noack, and B. Fahlke, *J. of Inclusion Phenomena*, **5**, 307 (1987).

Lovallo, M.C., A. Gouzinis, and M. Tsapatsis, *AIChE J.*, **44**, 1903 (1998).

May-Marom, A. and M.G. Katz, *J. Membr. Sci.* **27**, 119 (1986).

Mintova, S., J. Hedlund, V. Valtchev, B. Schoeman, and J. Sterte, *Chem. Commun.*, **15**, (1997).

Mintova, S., J. Hedlund, V. Valtchev, B. Schoeman, and J. Sterte, *J. Mater. Chem.*, **10**, 2217 (1998).

Nair, S., Z. Lai, V. Nikolakis, G. Xomeritakis, G. Bonilla, and M. Tsapatsis, *Micropor. Mesopor. Mater.*, **48**, 219, (2001).

NGK: http://www.ngk.co.jp, 2004.

NGK: *p*-Xylene production costs lowered significantly with new zeolite membrane, NGK Insulators in: Japan Chemical Week, Nov. 7th, 2002.

Noack, M., P. Kölsch, D. Fenzke, P. Toussaint, and J. Caro, *Micropor. Mater.* **3**, 201 (1994).

Noack, M. and J. Caro, in *Handbook of Porous Solids*, F. Schüth, K.S.W. Sing, J. Weitkamp (Eds.). Wiley-VCH, ISBN 3-527-30246-8, p. 2478, 2002.

Noack, M., P. Kölsch, R. Schäfer, P. Toussaint, and J. Caro, *Micropor. Mesopor. Mater.*, **49**, 25 (2001).

Noack, M., P. Kölsch, R. Schäfer, P. Toussaint, and J. Caro, *Chem. Eng. Technol.*, **25**, 221 (2002).

Noack, M., and B. Stelzer, unpublished, 2004.

Noack, M., P. Kölsch, V. Seefeld, P. Toussaint, G. Georgi, and J. Caro, *Micropor. Mesopor. Mater.*, **79**, 329 (2005).

Noack, M., G.T.P. Mabande, J. Caro, G. Georgi, W. Schwieger, P. Kölsch, and A. Avhale, *Micropor. Mesopor. Mater.*, **82**, 147 (2005).

Richter, H., I. Voigt, G. Fischer, and P. Puhlfürß, *Separ. Purific. Techn.*, **32**, 133 (2003).

Schäfer, R., M. Noack, P. Kölsch, M. Stöhr, and J. Caro, *Catal. Today*, **82**, 15 (2003).

Separion: http://www.separion.com, 2004.

Steriotis, Th.A., K.L. Stefanopoulos, A.Ch. Mitropoulos, and N.K. Kanellopoulos in *Recent advances in gas Separation by Microporous Ceramic Membranes*, N.K. Kanellopoulos (Ed.). Elsevier, ISBN 0-444-50272-6, p. 1, 2000.

Tanaka, Y., T. Tsuru, T. Yoshioka, and M. Asaeda, *Micropor. Mesopor. Mater.*, **54**, 257 (2002).

Tomita, T., K. Nakayama, and H. Sakai, *Micropor. Mesopor. Mater.*, **68**, 71 (2004).

Wang, Z. and Y. Yan, *Chem. Mater.*, **13**, 1101 (2001).

Wong, W.C., L.T.Y. Au, C.T. Ariso, and K.L. Yeung, *J. Membr. Sci.*, **193**, 141 (2001).

Xomeritakis, G., A. Gouzinis, S. Nair, T. Okubo, M. He, R.M. Overney, and M. Tsapatsis, *Chem. Engng Sci.*, **54**, 3521 (1999).